



HAL
open science

Autoregressive Modeling Approach for Non-stationary Vehicular Channel Simulation

Marwan Yusuf, Emmeric Tanghe, Frederic Challita, Pierre Laly, Luc Martens,
Davy Gaillot, M. Lienard, Wout Joseph

► **To cite this version:**

Marwan Yusuf, Emmeric Tanghe, Frederic Challita, Pierre Laly, Luc Martens, et al.. Autoregressive Modeling Approach for Non-stationary Vehicular Channel Simulation. IEEE Transactions on Vehicular Technology, 2022, 71 (2), pp.1124 - 1131. 10.1109/TVT.2021.3132859 . hal-03546025

HAL Id: hal-03546025

<https://hal.science/hal-03546025>

Submitted on 18 Aug 2023

HAL is a multi-disciplinary open access archive for the deposit and dissemination of scientific research documents, whether they are published or not. The documents may come from teaching and research institutions in France or abroad, or from public or private research centers.

L'archive ouverte pluridisciplinaire **HAL**, est destinée au dépôt et à la diffusion de documents scientifiques de niveau recherche, publiés ou non, émanant des établissements d'enseignement et de recherche français ou étrangers, des laboratoires publics ou privés.

Autoregressive Modeling Approach for Non-stationary Vehicular Channel Simulation

Marwan Yusuf, Emmeric Tanghe, Frederic Challita, Pierre Laly, Luc Martens,
Davy P. Gaillot, Martine Lienard, and Wout Joseph

Abstract—A framework is proposed for long-term vehicular channel simulation based on the vector time-frequency autoregressive (VTFAR) model for a sparse parametric description of nonstationary multivariate random processes. Based on vehicle-to-infrastructure tunnel measurements, we estimate the VTFAR model parameters and validate the model by comparing the parametric and non-parametric spectra of the measured channel in terms of the delay spread and stationarity time. In addition, the VTFAR model stability is investigated and an approximation for the correlated scattering channel is proposed. The experimental validation shows a good agreement with RMSE of only 0.01 for the delay spread and 0.4 for the stationarity time. This approach provides an efficient alternative for non-stationary channel simulation that is measurement-based and computationally inexpensive.

Index Terms—vehicular communication, channel modeling, autoregressive, non-stationary

I. INTRODUCTION

ONE of the key features of the envisioned intelligent transportation system (ITS) is connected vehicles. Such vehicles are expected to play a vital role in the information flow and communication in urban regions [1]. The mobile radio channel poses significant challenges to the design of communication systems due to time and frequency dispersions. An accurate and concise channel model to regenerate or predict the measured channel behavior is useful for channel simulation, performance evaluation, and further design of communication systems [2]. For this reason, modeling of mobile channels has received considerable attention. The early work of Bello [3] on randomly time-variant channels in characterizing the wide-sense stationary (WSS) and uncorrelated scattering (US) channel paved the way for several types of models. Statistical models, which have the advantage of reduced simulation times, have been widely adopted, and many have been developed for vehicle-to-vehicle (V2V) channels [4].

The WSSUS assumption simplifies the statistical characterization of linear time-varying (LTV) channels. However, this is not always fulfilled in practice, particularly in vehicular

scenarios. The author in [5] has shown that, in both single and multi-carrier systems, the WSS assumption in V2V channels simulation can lead to optimistic bit-error-rate (BER) results that are erroneous. In reality, power, delay, and Doppler associated with reflected multipath components (MPC) drift with time (WSS-violation), and channels show correlated scattering due to several MPCs that are close in the delay-Doppler domain reflecting off the same physical object (US-violation). In the literature, various approaches have been proposed to model the non-stationarity: 1) Tapped delay line (TDL) with different tap models depending on the delay spread and the BER statistics [6], 2) "birth/death" Markov process to account for the appearance and disappearance of taps [7], 3) stochastic modeling of the dynamic scatterers evolution and their delay and angular properties [8], or 4) geometry-based stochastic modeling (GSCM) that inherently includes the non-stationary behavior of the channel in the dynamic environment geometry [9]. Other approaches include deterministic modelling where site-specific scenarios are modelled e.g., using ray-tracing simulations [10] or artificial neural network (ANN) based channel modeling [11], which have more computational costs.

Another approach to describe the random fading process is parametric modeling [12]. Such models involve a parametric representation of an innovation system driven by white innovations noise. The statistics of the output process are then characterized by the parameters of the innovations system. Sparse (parsimonious, low-dimensional, low-rank) representations of the LTV radio channel have been widely used [13]. In this paper, we consider an autoregressive (AR) modeling approach for the accurate generation of non-stationary vector (multivariate) processes. This technique belongs to the class of parametric spectral estimation, and employs all-pole infinite-impulse response (IIR) filtering to shape the spectrum of uncorrelated Gaussian variates. An AR model is preferred over moving-average (MA) or hybrid ARMA models, as the variations of the mobile channel response resemble a correlated series with low peaks and deep fades [14]. An AR model for wideband indoor radio propagation was first presented in [15] and later applied to UWB channel modeling in [16] for indoor scenarios. Parametric modeling in the frequency domain is also investigated in [17] for WSSUS wideband and UWB channels.

Most existing non-stationary models were extended from their stationary counterpart. A vector time-frequency (VTF) AR model that describes non-WSSUS multivariate processes has been proposed in [18]. The frequency shifts (Doppler shifts), in addition to time shifts, provide an intuitive and physically motivated way of capturing the spectral and tem-

Marwan Yusuf, Emmeric Tanghe, Luc Martens and Wout Joseph are with the Department of Information Technology, Ghent University-imec, Belgium (e-mail: marwan.yusuf@ugent.be)

Frederic Challita, Pierre Laly, Davy P. Gaillot and Martine Lienard are with the Electronics Department - IEMN, TELICE group, University of Lille, France.

poral correlation of non-stationary vector processes without a severe loss in parsimony. The model is parsimonious for the practically relevant class of underspread vector processes (i.e., processes with rapidly decaying correlation in time and frequency). Based on a system of linear equations with a two-level block-Toeplitz (2LBT) structure, a VTFAR parameters estimator is also presented [18]. The contributions of this paper are summarized as follows.

- A framework for simulating a non-stationary TDL of a measured vehicular channel response using the VTFAR model approach is provided.
- The stability of the VTFAR model is investigated and an approximation for the correlated scattering channel is proposed.
- We investigate the parametric and non-parametric spectra of the channel and validate the model by comparing them in terms of the delay spread and the stationarity time.

The remainder of the paper is organized as follows. Section II briefly explains the VTFAR model and the parameters estimation. Section III presents the measurement campaign and the simulation framework for the measured channel response. Section IV discusses the correlated scattering channel and VTFAR model stability. Section V includes the model validation. Finally, conclusions are drawn in Section VI.

II. VTFAR MODELING

A. Non-WSSUS channel

The wireless channel is represented with a TDL as a random LTV system in the discrete form of

$$r[t] = \sum_{\tau} h[t, \tau] s[t - \tau]. \quad (1)$$

The received signal $r[t]$ is related to the transmit signal $s[t]$ via the 2-D channel impulse response (CIR) $h[t, \tau]$, where t is the time index and τ is the delay index. The CIR is a WSSUS random process when $h[t, \tau]$ is stationary with respect to t and mutually uncorrelated for different τ . The system can also be expressed in terms of frequency shifts by the spreading function $S_H[\nu, \tau] = \mathbb{F}_{t \rightarrow \nu} \{h[t, \tau]\}$ where \mathbb{F} is the Fourier transform and ν is the Doppler frequency index.

Generally, the correlation function $E\{S_H[\nu', \tau] S_H^*[\nu, \tau']\}$ that statistically characterizes the channel depends on four variables. For WSSUS, it simplifies to

$$E\{S_H[\nu', \tau] S_H^*[\nu, \tau']\} = C_H[\nu, \tau] \delta[\nu - \nu'] \delta[\tau - \tau'], \quad (2)$$

where $C_H[\nu, \tau]$ is known as the scattering function, i.e., the power spectral density of the WSSUS process. For non-WSSUS, this simplification is only valid within certain time and frequency intervals, known as the stationarity time T_s and stationarity bandwidth F_s , respectively [19]. The local scattering function (LSF) $C_H[t, f; \nu, \tau]$ becomes time and frequency dependent, which then describes the power of MPCs with delay τ and Doppler shift ν occurring at time t and frequency f [19]. This is true for doubly-underspread (DU) channels, a condition satisfied by most practical wireless radio channels. It means that the amount of delay-Doppler correlation has to

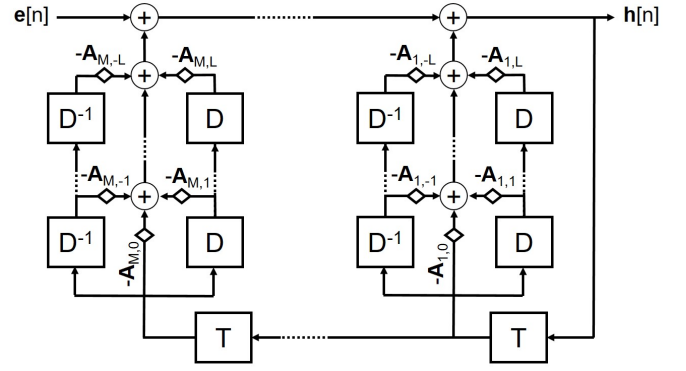


Fig. 1. Block diagram of the VTFAR model where T is a time shift operator, D is a Doppler shift operator, and the diamond shape is a matrix multiplication [18]

be smaller than the amount of delay-Doppler dispersion. In other words, only the neighboring MPCs are correlated [19].

The channel correlation function (CCF) is defined as the 4-D Fourier transform of the LSF

$$A_H[\Delta\nu, \Delta\tau; \Delta t, \Delta f] = \mathbb{F}_{t \rightarrow \Delta\nu} \mathbb{F}_{\tau \rightarrow \Delta\tau} \mathbb{F}^{-1}_{\nu \rightarrow \Delta t} \mathbb{F}^{-1}_{f \rightarrow \Delta f} \{C_H[t, f; \nu, \tau]\}. \quad (3)$$

The CCF characterizes the correlation of MPCs separated in time by Δt , in frequency by Δf , in delay by $\Delta\tau$, and in Doppler by $\Delta\nu$. The span of $\Delta\nu$ and $\Delta\tau$ wherein the CCF has significant correlation is what determines the T_s and F_s , respectively [19].

B. VTFAR model

The non-WSSUS channel can be described by an innovation system where the 2-D CIR is obtained by passing white innovations noise $\mathbf{e}[n]$ into a nonrandom LTV system $\mathbf{V}[n, m]$ as follows

$$\mathbf{h}[n] = \sum_m \mathbf{V}[n, m] \mathbf{e}[n - m]. \quad (4)$$

Here, the CIR is expressed in a vector form as $\mathbf{h}[n] = [h[n, 0] \dots h[n, \tau_m - 1]]^T$, where $n = 0, 1, \dots, N - 1$ is the innovations index, which can then be up-sampled to a desired sampling rate, i.e. $n = Kt$. This can be done as the channel variation is limited to slower Doppler rates. According to the VTFAR model [18], the innovations IIR filter $\mathbf{V}[n, m]$ is represented by Doppler shifts (l) in addition to the time shifts (m). Rewriting (4) in the VTFAR form gives

$$\mathbf{h}[n] = - \sum_{m=1}^M \sum_{l=-L}^L \mathbf{A}_{m,l} e^{j \frac{2\pi}{N} nl} \mathbf{h}[n - m] + \mathbf{e}[n], \quad (5)$$

where M and L denote the (temporal and spectral) model order, the $\tau_m \times \tau_m$ matrices $\mathbf{A}_{m,l}$ contain the AR model parameters, and $\mathbf{e}[n]$ is the complex Gaussian, temporally uncorrelated, circularly symmetric innovations noise vector with correlation matrix $E\{\mathbf{e}[n] \mathbf{e}^*[n']\} = \mathbf{C}[n] \delta(n - n')$. Fig. 1 represents the generation of the channel vector $\mathbf{h}[n]$ by passing the innovations noise vector $\mathbf{e}[n]$ through the recursive filter where time- and Doppler-shifted channel vectors are shaped

by the AR model parameters matrices $\mathbf{A}_{m,l}$. According to (5), elements of the $\mathbf{V}[n,m]$ matrices are constrained to lie in the subspace spanned by the complex exponentials with Doppler frequencies $l = -L, \dots, L$. A similar restriction is imposed on the innovations correlation matrix

$$\mathbf{C}[n] = \sum_{l=-2L}^{2L} \mathbf{C}_l e^{j\frac{2\pi}{N}nl}, \quad (6)$$

such that a matrix square root $\mathbf{C}^{1/2}[n]$ with Doppler order L can be found [18].

Another restriction in the VTFAR(M,L,B) is band-limiting the matrices $\mathbf{A}_{m,l}$ and \mathbf{C}_l , i.e. elements of these matrices with indices (τ, τ') are zero for $|\tau - \tau'| > B$, where B denotes the (one-sided) matrix bandwidth ($B \in \{0, 1, \dots, \tau_m - 1\}$). This is motivated by the fact that correlation decays with delay taps in DU channels (for US channels $B = 0$). Consequently, the number of parameters characterizing the banded VTFAR model is shown to be $\mathbb{N} = (M+1)(2L+1)(\tau_m(2B+1) - B(B+1))$ [18]. Thus, the parsimony of the VTFAR model is better for smaller M, L, τ_m , and B , making it particularly suited for the DU channels where $ML \ll N$. This plays an important role in developing computationally efficient parameter estimators for $\mathbf{A}_{m,l}$ and \mathbf{C}_l [18].

C. VTFAR parameters estimation

We consider the estimation of VTFAR model parameters from a single channel realization $\mathbf{h}[n]$ obtained from a measurement campaign. Estimation of the $\mathbf{A}_{m,l}$ involves solving a system of multichannel time-frequency Yule-Walker (TFYW) linear equations, similar to the classical YW equations. An approximation for the DU channels derived from (5) reads as follows [18]

$$\sum_{m=1}^M \sum_{l=-L}^L \mathbf{A}_{m,l} \mathbf{F}_h[m' - m, l' - l] = -\mathbf{F}_h[m', l'], \quad (7)$$

where $\mathbf{F}_h[m, l]$ is the average expected ambiguity function (EAF). Hence, the TFW equations express the EAF at a certain delay m' and Doppler l' as the linear combination of the EAF at different delay and Doppler values. In practice, the EAF is usually unknown and has to be estimated from a given observation of $\mathbf{h}[n]$. When multiple observations are available, the EAF can be estimated as [18]

$$\mathbf{F}_h[m, l] = \mathbb{E} \left\{ \sum_{n=0}^{N-1} \mathbf{h}[n] \mathbf{h}^*[n-m] e^{-j\frac{2\pi}{N}nl} \right\}. \quad (8)$$

In order to efficiently solve (7) for $\mathbf{A}_{m,l}$, the matrix equations are rewritten element-wise and re-stacked with a suitable order to reach a single matrix equation involving a 2LBT matrix as [18]

$$\mathbb{Z} \mathbf{a} = -\mathbf{z}. \quad (9)$$

Here, the matrices \mathbb{Z} and \mathbf{z} contain the $\mathbf{F}_h[m, l]$ elements, and \mathbf{a} contains the $\mathbf{A}_{m,l}$ elements. The 2LBT structure of \mathbb{Z} is the basis for a fast solution algorithm developed in [18], called the multichannel Wax-Kailath algorithm, from which the VTFAR parameters can be extracted. Once $\mathbf{A}_{m,l}$ are estimated, the



Fig. 2. Measurement campaign with the Tx in the tunnel and the Rx in the van

evaluation of the innovations matrices \mathbf{C}_l can be derived as [18]

$$\mathbf{C}_l = \frac{1}{N} \sum_{m=0}^M \sum_{l'=-L}^L \mathbf{A}_{m,l'} \mathbf{F}_h^*[m, l' - l]. \quad (10)$$

The correlation matrices $\mathbf{C}[n]$ can then be obtained from (6) via an iterative scheme that alternately enforces positive definiteness and Doppler and matrix band-limitations [18].

III. SIMULATION FRAMEWORK FOR VEHICULAR CHANNELS

In this section, we propose a framework for simulating vehicular radio channels using the VTFAR model. The parameters estimator requires at least one realization of the channel in order to calculate the EAF. The framework is thus applied to a CIR from a vehicle-to-infrastructure (V2I) measurement campaign that is briefly presented. As a long-term simulation, we use an 8 s duration of the measured channel, corresponding to approximately eight thousand snapshots over 900λ . This is much longer than the coherence time (40 ms from measurements [20]), thus ensuring a long-term scenario [19].

A. Measurement campaign

Measurements of a V2I scenario have been carried out in the Beveren tunnel in Belgium using the MIMOSA radio channel sounder [20]. The sounder uses 80 MHz of transmission bandwidth centered around a carrier frequency of 1.35 GHz. The transmitter (Tx) antenna is placed around the middle of the tunnel through an emergency exit door at a 2 m height. The receiver (Rx) antenna is mounted on the rooftop of a van carrying the Rx inside. The van moves through the tunnel at a 90 km/h speed, crossing the Tx position halfway. There was a medium traffic condition of 10-15 vehicles in the tunnel, many were trucks from the port of Antwerp. During the trip, the radio channel is sampled with a snapshot repetition time of 975.3 μ s, each with 819 frequency samples. The setup is shown in Fig. 2, and further details can be found in [20].

B. Proposed framework

1) *Pre-processing*: The channel sounder captures the channel transfer function (CTF) in the time and frequency domains.

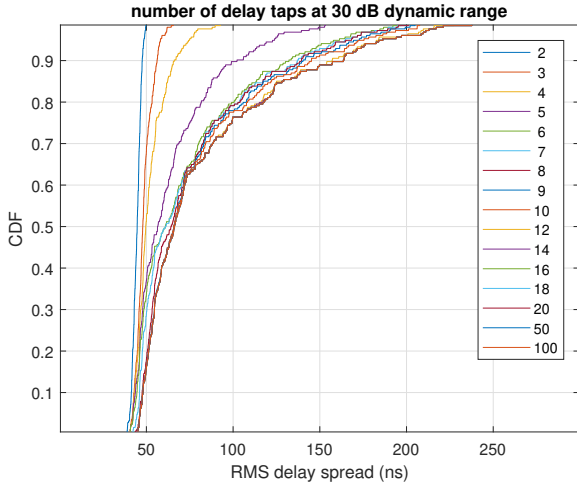


Fig. 3. CDF of the RMS delay spread for different number of taps

It includes both large-scale (path loss, shadowing,...) and small-scale fading effects. We first apply an inverse Fourier transform to the CTF using a Hann window to obtain the time-varying CIR. Then, we align the CIRs so that the maximum LOS components have the same absolute delay. Finally, we remove the large-scale fading using a moving-average filter with a window size of 10λ . This results in normalised CIRs that preserve the small-scale fading like what is commonly used for link-level simulations.

2) *Bandwidth*: The ITS spectrum for V2X communications supports direct low-latency connections over short distances, without the involvement of the cellular network. Standards like C-V2X and 802.11p can co-exist in the ITS spectrum by employing different channels within the band, where just 10 MHz of spectrum is required to support essential safety services [5], [21]. This makes V2X channels particularly suitable for the VTFAR model, since a small bandwidth means fewer delay taps and thus fewer model parameters. Consequently, we divide the measured CTF into 8 channels of 10 MHz bandwidth. The CIR is then calculated as mentioned above for each channel, from which the average EAF is estimated as in (8) by averaging over the 8 channels.

3) *Sampling rate*: The sampling rate used for link simulation and performance evaluation is typically orders of magnitude larger than physical Doppler frequencies, i.e. the delay tap processes are very narrowband. In that sense, a subsampled VTFAR model at an intermediate sampling rate that is close to the maximum Doppler frequency is followed by an optimum multistage interpolator in order to match the actual system sampling rate. In our scenario, the MPCs Doppler frequencies span up to 128 Hz. Thus, we sample the CIR at 256 Hz, which gives $\mathbf{h}[n]$.

4) *Number of taps*: The number of delay taps τ_m directly impacts the parsimony of the VTFAR model. It is desirable to include the minimum number of taps that is sufficient to model the channel. To that aim, we propose to set τ_m based on the second-order statistics of the channel, namely, the RMS delay and Doppler spreads. These parameters play a vital role in system performance and design, making them a relevant

TABLE I
KS-TEST P-VALUES OF THE DELAY AND DOPPLER SPREADS CDFS FOR DIFFERENT NUMBER OF TAPS

Taps	2	3	4	5	6	7	8
Delay	0	0	0	0	0.225	0.271	0.59
Doppler	0	0.005	0.06	0.225	0.225	0.81	0.98

criterion. Fig. 3 shows the CDF of the RMS delay spread for different number of delay taps. Only MPCs within 30 dB from the peak value are considered for calculating the delay spread. The 100-tap CDF represents the full channel since no MPCs exist beyond that. The CDF curves coincide for larger number of taps, since most of these large delay taps do not contain significant power. In order to decide on the number of taps, we use the two-sample Kolmogorov-Smirnov (KS) test and compare the p-values at 5% significance level. The test checks whether the spread of a certain τ_m comes from the same distribution as that of the full channel. The same procedure is done for the RMS Doppler spread, and the minimum number of taps whose spreads' distributions pass the tests is chosen to represent the channel. Table I shows the p-values for the delay and Doppler spreads at different number of taps, where it is clear that the distributions with 6 taps pass both tests.

IV. CORRELATED SCATTERING AND VTFAR STABILITY

In the previous section, we explained how to extract the CIR, calculate from it the average EAF $\mathbf{F}_h[m, l]$, and use it to estimate the matrices $\mathbf{A}_{m, l}$ and \mathbf{C}_l . We can then generate the channel coefficients $\mathbf{h}[n]$ by passing the innovations vector $\mathbf{e}[n]$ with the correlation matrix $\mathbf{C}[n]$ into the VTFAR model depicted in Fig. 1. However, the AR model is an IIR filter that is not guaranteed to be stable.

A. Stability analysis

A stable process is one that will not diverge to infinity (blow up). This means that the characteristic polynomial in the denominator of the transfer function vanishes only within the unit circle in the complex frequency plane (z -plane). From (5), the stability condition can be formulated as [22]

$$\det(\mathbf{I}_{\tau_m} + \mathbf{A}_{1, n} z^{-1} + \dots + \mathbf{A}_{M, n} z^{-M}) \neq 0 \quad \text{for } |z| \geq 1, \quad (11)$$

where $\mathbf{A}_{m, n} = \sum_{l=-L}^L \mathbf{A}_{m, l} e^{j2\frac{\pi}{N}nl}$ are the time-varying filter matrices at time n and \mathbf{I}_{τ_m} is a unitary matrix, all of size τ_m .

For the case of US channels ($B = 0$), all system matrices become diagonal. This means that the vector process $\mathbf{V}[n, m]$ can be modeled as τ_m scalar processes in parallel. This simplifies the stability condition, as the characteristic polynomial per process is now a scalar function rather than a matrix function. It is shown in [23] that such a system can be stabilized using an iterative algorithm based on the concept of root reflection/shrinkage known from the time-invariant case by applying it to the time-varying instantaneous roots of (11).

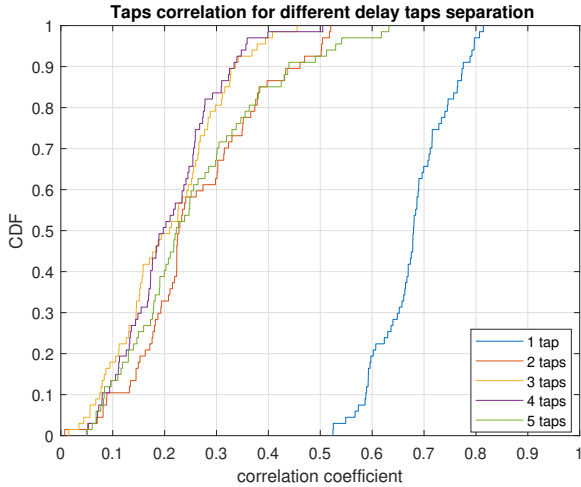


Fig. 4. CDF of the correlation coefficient for different taps separation

B. Correlation analysis

According to [24], the observed fading process in vehicular channels shows a much stronger violation of the WSS assumption than the US one. Channels show correlated scattering due to several MPCs that are close in the delay-Doppler domain reflecting off the same physical object, or leakage due to bandwidth/time limitations at Tx or Rx. This happens when the signal's bandwidth is larger than the stationarity bandwidth. It is observed in [24] that the stationarity bandwidths from a large set of measurements in different vehicular scenarios are above 150 MHz on average. This is very much larger than the required 10 MHz communication bandwidth for V2X systems. It is thus expected that the taps correlation will not be significant in our scenario.

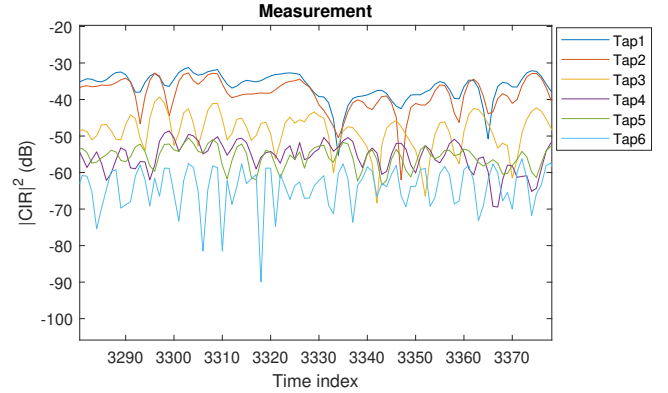
We investigate the correlation as a function of the delay taps separation. Fig. 4 shows the CDF of the correlation coefficient between delay taps up to 5 taps apart. It is clear that a correlation of 0.7 on average can be found only with the adjacent tap, while taps separated by two taps or more have insignificant correlation (below 0.3 on average). Moreover, it shows that there is no much variation around the mean value, only a standard deviation of 0.07 for the adjacent tap.

C. Correlation approximation for stable modeling

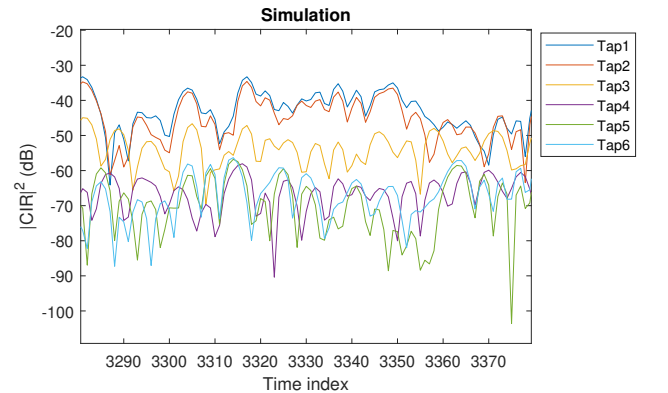
In order to simulate the correlated scattering channel with a stable AR model, we propose to set $B = 0$, resulting in a diagonal (uncorrelated) matrices $\mathbf{A}_{m,n}$ and $\mathbf{C}[n]$. The model can now be stabilized as aforementioned in the US case. Then, we approximate the taps correlation to the mean value, since its time-variation is limited as depicted in Fig. 4. The correlation is introduced to the innovations matrix as follows

$$\hat{\mathbf{C}}[n] = \mathbf{C}^{1/2}[n] \mathbf{R} \mathbf{C}^{1/2}[n], \quad (12)$$

where \mathbf{R} is the $\tau_m \times \tau_m$ correlation matrix calculated from the measurements by averaging over the total duration. In other words, instead of passing uncorrelated multivariate innovations, $\mathbf{e}[n]$ are now correlated based on \mathbf{R} , thus $\hat{\mathbf{C}}[n]$ is no longer diagonal.



(a)



(b)

Fig. 5. CIR power in dB from measurements (a) and simulation (b)

We simulate the 6-tap channel with the proposed approximation, where the model orders (M, L) per tap are estimated using the minimum description length information criterion presented in [23]. The simulated channel is upsampled to have the same sampling rate as the measurement, i.e. $K = 4$. Fig. 5 compares segments of the CIR power from both measurements and simulation. It clearly shows that the model generates a stable process that resembles the measured channel. To check the validity of the correlation approximation, we compare the measured and simulated 1-tap separation correlation coefficient, which is the most significant one. Fig. 6 shows that the correlation of the generated channel approximates that of the measurement quite well over a long duration with RMSE of 0.08.

V. MODEL VALIDATION

Non-stationary channels can be characterized by the LSF, which is the time-varying second order statistics of the channel. We validate the VTFAR model by comparing the parametric LSF of the model to a non-parametric LSF calculated from the measurement.

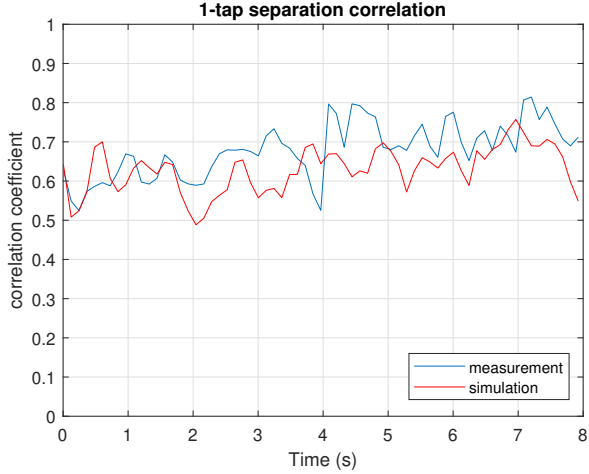


Fig. 6. 1-tap separation correlation coefficient from measurements and simulation

A. Parametric vs. non-parametric spectra

Since we are more interested in the non-WSS nature of the channel, we discard the LSF's dependency on frequency and only consider the time dependency. This makes the LSF a 3D function in time, delay and Doppler. The time evolution can be investigated by projecting the LSF on the delay and Doppler domains, resulting in the delay and Doppler power profiles or spectra. The model validation is based on comparing the spectra estimated from a non-parametric multitapers approach as in [25], to the parametric spectra of the VTFAR model. According to [18], the parametric LSF is expressed as

$$\hat{C}_H[n; \nu, \tau] = \frac{\hat{\mathbf{C}}[n]}{\left| \mathbb{F}_{l \rightarrow n}^{-1} \mathbb{F}_{m \rightarrow \nu} \{ \mathbf{A}_{m,l} \} \right|^2}. \quad (13)$$

Fig. 7 shows the parametric spectra versus the non-parametric spectra for an 8 s duration of the 6-tap channel. The parametric spectra are evaluated by summing the LSF from (13) in the delay and Doppler dimensions. The details of estimating the non-parametric spectra from the measurement can be found in [20]. The finite-dimensional spaces of the parametric model can be clearly noticed in the smooth nature of its spectra, compared to the sample-based non-parametric spectra. Nonetheless, we notice the similarity between the two spectra in both delay and Doppler domains. The power-delay profiles are aligned to have the LOS component at zero delay as discussed in the pre-processing step, while the Doppler spectra show the LOS component's shift from positive to negative Doppler frequencies as the Rx crosses the Tx position in the tunnel (Section III-A).

B. Comparing spectra for model validation

We validate the model by investigating how well it matches the time-varying behaviour of the non-stationary channel. Hence, we compare the parametric and non-parametric spectra on two levels: the channel's coherence level, represented by the delay spread, and the channel's stationarity level, represented by the stationarity time. While the delay spread measures the

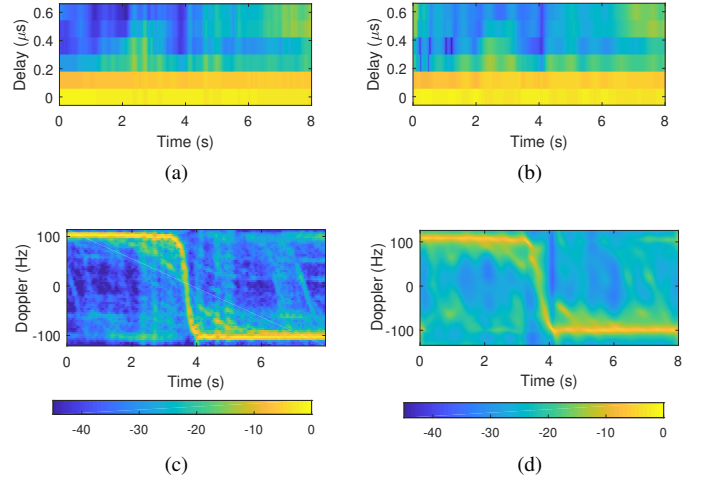


Fig. 7. Non-parametric power profiles in delay (a) and Doppler (c) versus the parametric profiles in delay (b) and Doppler (d) in dB

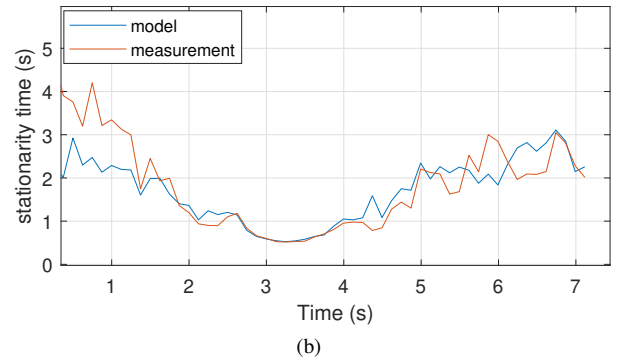
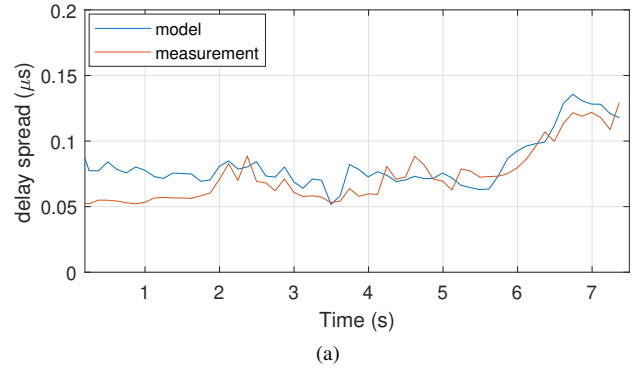


Fig. 8. Model validation in terms of the RMS delay spread (a) and stationarity time (b)

time dispersion of the channel, which may cause inter-symbol interference, the stationarity time measures how often this dispersion varies in time. The stationarity time is estimated as $T_s = 1/\hat{s}_{\Delta\nu}$ [25] where

$$\hat{s}_{\Delta\nu} = \frac{1}{\|A_H\|_1} \sum_{\Delta\nu} \sum_{\Delta f} \sum_{\Delta t} |\Delta\nu| |A_H[\Delta\nu; \Delta t, \Delta f]| \quad (14)$$

is the the CCF Doppler moment and $\|\cdot\|_1$ is the $L_{1,1}$ norm.

For validation, we compare the time evolution of both parameters to measure how well the model matches the time-

varying behaviour of the channel. Fig. 8 shows the RMS delay spread and stationarity time for the parametric vs. non-parametric spectra. We discard the first second to provide enough initialization time for the IIR filter's transient response to settle [26]. We see that both parameters show great similarity between the two spectra. We quantify the RMSE to be 0.01 for the delay spread and 0.4 for the stationarity time. The discrepancy between the curves of the stationarity time and delay spread can be attributed to the difference between the two types of spectra. The non-parametric spectrum estimation methods usually have higher variance and fluctuation rate than the parametric spectrum estimation ones [27]. This can be clearly seen in the spectra plotted in Fig. 7.

VI. CONCLUSION

Parametric modeling of non-stationary processes is applied to simulate a measured V2I channel in a tunnel in Belgium. We propose a framework for long-term simulation based on the vector time-frequency autoregressive (VTFAR) model. We analyse the stability of the model and propose an approximation for the correlated scattering channel that guarantees stability. A 6-tap channel is simulated based on the measurement, where the VTFAR model parameters are estimated using the proposed approach. Moreover, the parametric spectra of the model are compared to non-parametric spectra of the measured channel. We validate the model in terms of the delay spread and stationarity time. The model is found to simulate the measured channel very well with RMSE of 0.01 for the delay spread and 0.4 for the stationarity time. This measurement-based and computationally inexpensive approach provides an efficient alternative for non-stationary channel simulations. A future research direction is to include more scenarios (different environments, multiple antennas, etc.) and study the parameterization dependency of the model as well as the filter's initiation transient behaviour. In addition, comparing the model's complexity and performance to similar recent approaches can be very beneficial (e.g. [11]).

ACKNOWLEDGMENT

The author would like to thank Dr. Michael Jachan (Brain Products GmbH.) for his help and advice with the software implementation of this work.

REFERENCES

- [1] ETSI, "Intelligent transport systems (ITS); vehicular communications; basic set of applications; definitions," *Tech. Rep. ETSI TR 102 6382009*, Jun. 2009.
- [2] C. F. Mecklenbrauker, A. F. Molisch, J. Karedal, F. Tufvesson, A. Paiar, L. Bernado, T. Zemen, O. Klemp, and N. Czink, "Vehicular channel characterization and its implications for wireless system design and performance," *Proceedings of the IEEE*, vol. 99, no. 7, pp. 1189–1212, Jul. 2011.
- [3] P. Bello, "Characterization of randomly time-variant linear channels," *IEEE Transactions on Communications Systems*, vol. 11, no. 4, pp. 360–393, Dec. 1963.
- [4] A. F. Molisch, F. Tufvesson, J. Karedal, and C. F. Mecklenbrauker, "A survey on vehicle-to-vehicle propagation channels," *IEEE Wireless Communications*, vol. 16, no. 6, pp. 12–22, Dec. 2009.
- [5] D. W. Matolak, "Channel modeling for vehicle-to-vehicle communications," *IEEE Communications Magazine*, vol. 46, no. 5, pp. 76–83, May 2008.

- [6] G. Acosta-Marum and M. A. Ingram, "A BER-based partitioned model for a 2.4 GHz vehicle-to-vehicle expressway channel," *Wireless Personal Communications*, vol. 37, no. 3-4, pp. 421–443, May 2006.
- [7] I. Sen and D. W. Matolak, "Vehicle-vehicle channel models for the 5-GHz band," *IEEE Transactions on Intelligent Transportation Systems*, vol. 9, no. 2, pp. 235–245, Jun. 2008.
- [8] R. He, O. Renaudin, V.-M. Kolmonen, K. Haneda, Z. Zhong, B. Ai, and C. Oestges, "A dynamic wideband directional channel model for vehicle-to-vehicle communications," *IEEE Transactions on Industrial Electronics*, vol. 62, no. 12, pp. 7870–7882, Dec. 2015.
- [9] R. He, B. Ai, G. L. Stüber, and Z. Zhong, "Mobility model-based non-stationary mobile-to-mobile channel modeling," *IEEE Transactions on Wireless Communications*, vol. 17, no. 7, pp. 4388–4400, Jul. 2018.
- [10] Y. Zhang, J. Sun, G. Gui, H. Gacanin, and H. Sari, "A generalized channel dataset generator for 5G new radio systems based on ray-tracing," *IEEE Wireless Communications Letters*, pp. 1–1, Aug. 2021.
- [11] X. Zhao, F. Du, S. Geng, Z. Fu, Z. Wang, Y. Zhang, Z. Zhou, L. Zhang, and L. Yang, "Playback of 5G and beyond measured MIMO channels by an ANN-based modeling and simulation framework," *IEEE Journal on Selected Areas in Communications*, vol. 38, no. 9, pp. 1945–1954, Sept. 2020.
- [12] K. Baddour and N. Beaulieu, "Autoregressive modeling for fading channel simulation," *IEEE Transactions on Wireless Communications*, vol. 4, no. 4, pp. 1650–1662, Jul. 2005.
- [13] G. Matz and F. Hlawatsch, "Time-varying communication channels: Fundamentals, recent developments, and open problems," in *2006 14th European Signal Processing Conference*, Sept. 2006, pp. 1–5.
- [14] T. C. Mills, *Applied time series analysis: A practical guide to modeling and forecasting*. Academic press, Jan. 2019.
- [15] S. Howard and K. Pahlavan, "Autoregressive modeling of wide-band indoor radio propagation," *IEEE Transactions on Communications*, vol. 40, no. 9, pp. 1540–1552, Sep. 1992.
- [16] S. Ghassemzadeh, R. Jana, C. Rice, W. Turin, and V. Tarokh, "Measurement and modeling of an ultra-wide bandwidth indoor channel," *IEEE Transactions on Communications*, vol. 52, no. 10, pp. 1786–1796, Oct. 2004.
- [17] G. Gu, X. Gao, J. He, and M. Naraghi-Pour, "Parametric modeling of wideband and ultrawideband channels in frequency domain," *IEEE Transactions on Vehicular Technology*, vol. 56, no. 4, pp. 1600–1612, Jul. 2007.
- [18] M. Jachan, G. Matz, and F. Hlawatsch, "Vector time-frequency AR models for nonstationary multivariate random processes," *IEEE Transactions on Signal Processing*, vol. 57, no. 12, pp. 4646–4659, Dec. 2009.
- [19] G. Matz, "On non-WSSUS wireless fading channels," *IEEE Transactions on Wireless Communications*, vol. 4, no. 5, pp. 2465–2478, Sep. 2005.
- [20] M. Yusuf, E. Tanghe, P. Laly, F. Challita, B. Lannoo, R. Halili, R. Berkmans, M. Weyn, L. Martens, D. P. Gaillot, M. Liénard, and W. Joseph, "Experimental study on the impact of antenna characteristics on non-stationary V2I channel parameters in tunnels," *IEEE Transactions on Vehicular Technology*, vol. 69, no. 11, pp. 12 396–12 407, Nov. 2020.
- [21] V. Mannoni, V. Berg, S. Sesia, and E. Perraud, "A comparison of the V2X communication systems: ITS-G5 and C-V2X," in *2019 IEEE 89th Vehicular Technology Conference (VTC2019-Spring)*, Apr. 2019, pp. 1–5.
- [22] H. Lütkepohl, *New introduction to multiple time series analysis*. Springer Science & Business Media, Mar. 2005.
- [23] M. Jachan, G. Matz, and F. Hlawatsch, "TFARMA models: order estimation and stabilization," in *Proceedings. (ICASSP '05). IEEE International Conference on Acoustics, Speech, and Signal Processing, 2005.*, vol. 4, Mar. 2005, pp. iv/301–iv/304 Vol. 4.
- [24] L. Bernadó, T. Zemen, F. Tufvesson, A. F. Molisch, and C. F. Mecklenbrauker, "The (in-) validity of the WSSUS assumption in vehicular radio channels," in *2012 IEEE 23rd International Symposium on Personal, Indoor and Mobile Radio Communications - (PIMRC)*, Sep. 2012, pp. 1757–1762.
- [25] M. Yusuf, E. Tanghe, F. Challita, P. Laly, D. P. Gaillot, M. Liénard, L. Martens, and W. Joseph, "Stationarity analysis of V2I radio channel in a suburban environment," *IEEE Transactions on Vehicular Technology*, vol. 68, no. 12, pp. 11 532–11 542, Dec. 2019.
- [26] V. Valimaki and T. Laakso, "Suppression of transients in variable recursive digital filters with a novel and efficient cancellation method," *IEEE Transactions on Signal Processing*, vol. 46, no. 12, pp. 3408–3414, Dec. 1998.

- [27] Zhao, Hangfang and Gui, Lin, "Nonparametric and parametric methods of spectral analysis," *MATEC Web Conf.*, vol. 283, p. 07002, June 2019. [Online]. Available: <https://doi.org/10.1051/mateconf/201928307002>